Magnetotransport in the doped Mott insulator

Ekkehard Lange and Gabriel Kotliar
Serin Physics Laboratory, Rutgers University, 136 Frelinghuysen Road, Piscataway, New Jersey 08854
(Received 11 March 1998)

We investigate the Hall effect and the magnetoresistance of strongly correlated electron systems using the dynamical mean-field theory. We treat the low- and high-temperature limits analytically, and explore some aspects of the intermediate-temperature regime numerically. We observe that a bipartite-lattice condition is responsible for the high-temperature result $\sigma_{xy}\sim 1/T^2$ obtained by various authors, whereas the generic behavior is $\sigma_{xy}\sim 1/T$, as for the longitudinal conductivity. We find that Kohler's rule is obeyed neither at high nor at intermediate temperatures. [S0163-1829(99)06203-7]

I. INTRODUCTION

The Hubbard model[1–3] of strongly correlated electron systems has been an enduring problem in condensed-matter theory. It is believed to capture some of the anomalous physics of heavy-fermion systems and high-T_c superconductors.[4] Its crucial feature is the interplay of itineracy and a local interaction U that is either comparable with or much greater than the bare bandwidth.

In this paper, we investigate the impact of a magnetic field on the charge transport in strongly correlated electron systems within the Hubbard model. This issue involves different quantities that are closely related, and should therefore be considered within the *same* approximation scheme. We meet this condition by using the dynamical mean-field theory which becomes exact in the limit of infinite dimensions. A major though nontrivial simplification of this approach is that transport properties are described solely by the single-particle spectrum.[5–8] While the dynamical mean-field theory still captures many properties of real three-dimensional transition-metal oxides, it fails to describe cuprate superconductors equally well, mainly because it does not properly take into account magnetic correlations. Nevertheless, it is important to explore this approximation scheme fully in order to establish a sound starting point for future improvements.

The Hall constant of the single-band Hubbard model has already been considered within the dynamical mean-field theory by Pruschke, Jarrell, and Freericks[8] and Majumdar and Krishnamurthy.[9] The former authors computed the Hall constant and Hall angle as functions of temperature for various doping levels at—in our units—$U=2\sqrt{2}D$(D is the half-bandwidth) using the noncrossing approximation (NCA) and a quantum Monte Carlo (QMC) technique to solve the single-impurity problem. Majumdar and Krishnamurthy mainly focused on the relation between the infinite-frequency Hall constant investigated by Shastry, Shraiman and Singh,[10] and the dc Hall constant, using the iterated-perturbation theory (IPT) of Ref. 11.

In addition to the Hall effect and the ordinary resistivity, we investigate the magnetoresistance. We tie our numerical analysis at intermediate temperatures to analytical results valid in the low- and high-temperature limits. This allows to disentangle the coherent and incoherent contributions of the single-particle spectrum to the magnetotransport and to gain some understanding of either. We always mainly focus on the parameter regime close to the density-driven Mott transition. This paper is organized as follows: In Sec. II, we briefly summarize the dynamical mean-field theory within the single-band Hubbard model, and derive expressions for the quantities to be calculated. Then, by using a Fermi-liquid parametrization for the spectral function, we examine all quantities in the low-temperature regime (Sec. III), and study their dependences on temperature and on the doping level. Moreover, we discuss the impact of correlations close to half-filling. In Sec. IV, we employ a recently developed scheme to expand transport coefficients in powers of $1/T$ (Ref. 12) within the $U=\infty$ Hubbard model to study the opposite limit of high temperatures. We show that the high-temperature behaviors of the Hall constant and Hall angle can be affected by specific lattice symmetries, and that the Hall angle increases at most linearly with temperature. Then we explore the intermediate-temperature regime numerically (Sec. V) by either using the NCA or the IPT, depending on whether our focus is more on higher or lower temperatures, respectively. Finally, in Sec. VI, we summarize and discuss our results.

II. FORMALISM

We consider the N_s-fold degenerate Hubbard model

$$H=-t\sum_{\langle ij\rangle\sigma} c_{i\sigma}^{+}c_{j\sigma}+\frac{U}{2}\sum_{i\sigma\neq\sigma'} n_{i\sigma}n_{i\sigma'}, \tag{1}$$

where, in the first term, the sum is over nearest neighbors. The index σ can be thought of as a spin or an orbital index, and will run from 1 to N_s. For a single band, $N_s=2$. In the limit of infinite spatial dimensions, $d\to\infty$, the irreducible self-energy and all vertex functions collapse onto a single site.[5,13] As a consequence, these functions no longer depend on momentum. This, in turn, implies that all vertex corrections of the conductivity tensor vanish,[6–8] which therefore can be calculated from the single-particle spectral function

$$A(\omega,\vec{\epsilon_k})=-\frac{1}{\pi}\mathrm{Im}G(\omega,\vec{\epsilon_k}). \tag{2}$$

Here $G(\omega,\vec{\epsilon_k})$ is the retarded Green's function,

$$G(\omega,\epsilon_{\vec{k}})=\frac{1}{\omega+\mu-\epsilon_{\vec{k}}-\Sigma(\omega)}, \tag{3}$$

where μ is the chemical potential and $\Sigma(\omega)$ is the momentum-independent self-energy. The Green's function (3) must be calculated by solving a single-impurity Anderson model supplemented by a self-consistency condition.[7] In terms of the spectral function (2), the ordinary conductivity, the Hall conductivity, and the magnetoconductance read:[14]

$$\sigma_{xx}=N_s\pi e^2\int d\epsilon\,\phi_{xx}(\epsilon)\int d\omega\left[-\frac{\partial f(\omega)}{\partial\omega}\right]A(\omega,\epsilon)^2, \tag{4}$$

$$\sigma_{xy}=\frac{N_s 2\pi^2 e^3 H}{3}\int d\epsilon\,\phi_{xy}(\epsilon)\int d\omega\left[-\frac{\partial f(\omega)}{\partial\omega}\right]A(\omega,\epsilon)^3, \tag{5}$$

$$\Delta\sigma_{xx}=\frac{N_s 2\pi^3 e^4 H^2}{5}\int d\epsilon\,\phi_M(\epsilon)\int d\omega\left[-\frac{\partial f(\omega)}{\partial\omega}\right]A(\omega,\epsilon)^4. \tag{6}$$

Here H is the magnetic field and e denotes the charge of an electron, hence $e<0$. Furthermore, $f(\omega)=1/[\exp(\beta\omega)+1]$ is the Fermi function, where $\beta=1/T$ is the inverse temperature. Since the spectral function depends on $\vec{k}$ only via the band dispersion $\epsilon_{\vec{k}}$, we could write all sums over the Brillouin zone as integrals over the following transport functions:

$$\phi_{xx}(\epsilon)=\frac{1}{N}\sum_{\vec{k}}(\epsilon^x_{\vec{k}})^2\,\delta(\epsilon-\epsilon_{\vec{k}}), \tag{7}$$

$$\phi_{xy}(\epsilon)=\frac{1}{N}\sum_{\vec{k}}\det(\vec{k})\,\delta(\epsilon-\epsilon_{\vec{k}}), \tag{8}$$

$$\phi_M(\epsilon)=\frac{1}{N}\sum_{\vec{k}}M(\vec{k})\,\delta(\epsilon-\epsilon_{\vec{k}}). \tag{9}$$

Here N denotes the total number of lattice sites. Upper indices indicate differentiations with respect to a component of the Bloch vector such as in, say,

$$\epsilon^x_{\vec{k}}=\frac{\partial\epsilon_{\vec{k}}}{\partial k_x}. \tag{10}$$

Finally, the integrands of Eqs. (8) and (9) contain the functions

$$\det(\vec{k})=\begin{vmatrix}\epsilon^x_{\vec{k}}\epsilon^x_{\vec{k}} & \epsilon^{xy}_{\vec{k}}\\ \epsilon^y_{\vec{k}}\epsilon^x_{\vec{k}} & \epsilon^{yy}_{\vec{k}}\end{vmatrix}, \tag{11}$$

$$M(\vec{k})=\epsilon^{xxx}_{\vec{k}}\epsilon^x_{\vec{k}}(\epsilon^y_{\vec{k}})^2-2\epsilon^{xxy}_{\vec{k}}(\epsilon^x_{\vec{k}})^2\epsilon^y_{\vec{k}}+\epsilon^{xyy}_{\vec{k}}(\epsilon^x_{\vec{k}})^3 -(\epsilon^x_{\vec{k}})^2[\epsilon^{xx}_{\vec{k}}\epsilon^{yy}_{\vec{k}}-(\epsilon^{xy}_{\vec{k}})^2]. \tag{12}$$

On a hypercubic lattice in d dimensions,

$$\epsilon_{\vec{k}}=-\frac{2t}{\sqrt{2d}}\sum_{i=1}^{d}\cos(k_i a). \tag{13}$$

Henceforth, we set the lattice spacing a and the half-bandwidth $D\equiv 2t$ equal to 1. For the band of Eq. (13), the noninteracting density of states, $D(\epsilon)$, and the transport functions (7)–(9) can easily be calculated to be

$$D(\epsilon)=\sqrt{2/\pi}e^{-2\epsilon^2}, \tag{14}$$

$$\phi_{xx}(\epsilon)=\frac{1}{4d}D(\epsilon), \tag{15}$$

$$\phi_{xy}(\epsilon)=-\frac{1}{4d^2}\epsilon D(\epsilon), \tag{16}$$

$$\phi_M(\epsilon)=-\frac{1}{16d^2}D(\epsilon). \tag{17}$$

Obviously, σ_{xx}, σ_{xy}, and $\Delta\sigma_{xx}$ are of the orders $1/d$, $1/d^2$, and $1/d^2$, respectively. Consequently, the Hall constant and the magnetoresistance are of zeroth order in d, and are given by

$$R_H=\frac{\sigma_{xy}}{\sigma_{xx}^2 H}, \tag{18}$$

$$\Delta\rho=-\frac{\Delta\sigma_{xx}}{\sigma_{xx}^2} \tag{19}$$

as $d\to\infty$, respectively. Equations (6), (17), and (19) imply that the magnetoresistance is strictly non-negative in infinite dimensions. This means that the coupling of the magnetic field to the orbital motion of the electrons enhances the resistivity. At any finite dimension, there is an additional contribution from the Hall conductivity to the magnetoresistance which is of opposite sign, $\Delta\rho=-\rho^2(\Delta\sigma_{xx}+\rho\sigma_{xy}^2)$, where $\rho=1/\sigma_{xx}$. In this work, rather than using the Gaussian density of states (14), we choose the semicircular one,

$$D(\epsilon)=\frac{2}{\pi}\Theta(1-|\epsilon|)\sqrt{1-\epsilon^2}, \tag{20}$$

since then the ϵ integrals in Eqs. (4)–(6) can be performed analytically. Here $\Theta(x)$ is the Heaviside function, which is either 1 or 0 depending on whether x is greater or smaller than 0, respectively.

To calculate the spectral function (2), we employ two methods: At low temperatures, we use the IPT modified for finite doping levels as described in Ref. 11. This method becomes exact in various limits at zero temperature, and has been extended to finite temperatures in Ref. 15. At high temperatures, we use the NCA for the infinite-U case.[16] This approach has been shown to give results which are in good agreement with both QMC (Ref. 17) and numerical renormalization-group calculations[18] at high temperatures.

Before proceeding, we discuss the relevant energy scales. We are primarily interested in the physics close to half-filling, $\delta\to 0$, where $n=1-\delta$ denotes the average occupancy per lattice site. To understand the physics in this regime, we employ the relation of the dynamical mean-field theory to the single-impurity Anderson model. For $\delta\ll 1$, we are in the local-moment regime, and an Abrikosov-Suhl resonance shows up in the local spectral function

$$A(\omega)=\int_{-\infty}^{\infty} d\epsilon\, D(\epsilon)A(\omega,\epsilon) \tag{21}$$

for low enough temperatures. Its width defines an energy scale T^*,[19,20] which is not to be confused with the quasiparticle damping [Eq. (23)] that we will introduce further down. The emergence of a resonance at the Fermi level indicates a Kondo-like screening of the local moment. In fact, the local-spin susceptibility crosses over from local- to screened-moment behavior at a ''Kondo temperature'' $T_{\rm coh}$.[19,20] $T_{\rm coh}$ defines the coherence temperature below which Fermi-liquid theory is applicable.[20] Generally, $T_{\rm coh}\ll T^*$. The emergence of two low-energy scales is known from Kondo-lattice systems.[21] Finally, our high-energy scale is D, since we are only interested in temperatures much smaller than the Mott-Hubbard gap, $T\ll U$.

For temperatures most pertinent to experiments, the magnetotransport is governed by both the coherence peak and the incoherent backround of the spectrum. It is of fundamental interest to separate both contributions. In the Fermi-liquid regime, the transport is entirely determined by the coherence peak, and our analysis of Sec. III addresses its contribution only. Our high-temperature analysis of Sec. IV, on the other hand, captures the contribution of the completely incoherent lower Hubbard band to the magnetotransport.

III. LOW-TEMPERATURE LIMIT

At very low temperatures, Fermi-liquid theory applies. Then the Green's function (3) can be approximated by expanding the self-energy to second order in ω, thus capturing finite-lifetime effects of the quasiparticles:

$$\Sigma(\omega)=(1-1/Z)\omega+\alpha\omega^2+i\gamma(\omega). \tag{22}$$

Here, $Z=[1-\partial\,\mathrm{Re}\Sigma(\omega)/\partial\omega|_{\omega=0}]^{-1}$ is the quasiparticle residue at the Fermi level, and $\alpha=\frac{1}{2}\partial^2\,\mathrm{Re}\Sigma(\omega)/\partial\omega^2|_{\omega=0}$. Moreover,

$$\gamma(\omega)=\tilde{\gamma}[T^2+(\omega/\pi)^2]\equiv\gamma_0(T)[1+(\beta\omega/\pi)^2] \tag{23}$$

is the quasiparticle damping. Due to Eq. (22), the spectral function becomes

$$A(\omega,\epsilon)=L_{\gamma(\omega)}\left(\frac{\omega}{Z}-\alpha\omega^2+\tilde{\mu}-\epsilon\right), \tag{24}$$

where $L_\Gamma(\omega)=(1/\pi)[\Gamma/(\Gamma^2+\omega^2)]$ is the Lorentzian normalized to unity, and $\tilde{\mu}=\mu-\mathrm{Re}\Sigma(0)$ is the effective chemical potential. In the limits $\omega\to0$ and $T\to0$, Eq. (24) reduces to the correct result, $\lim_{\omega\to0}\lim_{T\to0}A(\omega,\epsilon)=\delta(\epsilon-\tilde{\mu})$.[22] Using also the sum rules $\int_{-\infty}^{\infty}d\epsilon\,[L_\Gamma(\epsilon)]^{n+1}=(2n-1)!!/(2\pi\Gamma)^n n!$ for integer n, and the fact that the width of $L_\Gamma(\epsilon)$ is $1/\tau=2\Gamma$, we can check that Eqs. (4)–(6) reduce to the standard Boltzmann-theory results as $T\to0$. Since $A(\omega,\epsilon)$ of Eq. (24) is only the low-frequency part of the spectral function, it only carries a small fraction of the total spectral weight determined by the sum rule. When calculating transport coefficients, this does not matter: Incoherent contributions missing in Eq. (24) are cut off by $-\partial f(\omega)/\partial\omega$.

Before proceeding, we investigate how the quasiparticle damping depends on the correlation strength. From Eqs. (20), (21), and (24), we obtain the width of the Abrikosov-Suhl resonance:

$$T^*\simeq ZD. \tag{25}$$

T^* is a measure for the Fermi energy of the quasiparticles. At zero temperature, T^* is the only energy scale in the problem. Then, the self-energy is given by $\Sigma(\omega)=a\omega/T^*+ib(\omega/T^*)^2$ for $\omega\ll T^*$, with some constants a and b. By comparing this expression to the Fermi-liquid expansion (22), we find $1/T^*\propto1-1/Z$ and $\tilde{\gamma}\propto1/T^{*2}$. The former relation is consistent with Eq. (25) since in the vicinity of the density-driven Mott transition, $Z\sim\delta$.[20] By inserting the other relation $\tilde{\gamma}\propto1/T^{*2}$ into the definition of γ_0 in Eq. (23), and by also using Eq. (25), we obtain

$$\gamma_0=A\frac{T^2}{Z^2D}, \tag{26}$$

where A is a dimensionless number and which is valid close to the density-driven Mott transition.

Using Eqs. (23) and (24), we find that to leading order in T, the conductivities (4)–(6) do not depend on α:

$$\sigma_{xx}=\frac{N_s e^2}{2\gamma_0}\phi_{xx}(\tilde{\mu})E^{(1)}, \tag{27}$$

$$\sigma_{xy}=\frac{N_s e^3 H}{4\gamma_0^2}\phi_{xy}(\tilde{\mu})E^{(2)}, \tag{28}$$

$$\Delta\sigma_{xx}=\frac{N_s e^4 H^2}{8\gamma_0^3}\phi_M(\tilde{\mu})E^{(3)}, \tag{29}$$

where the numbers $E^{(l)}$ are given by

$$E^{(l)}=\int_{-\infty}^{\infty}\frac{dx}{4\cosh^2\left(\frac{x}{2}\right)\left[1+\left(\frac{x}{\pi}\right)^2\right]^l}. \tag{30}$$

Numerically, we obtain $E^{(1)}=0.822\,467$, $E^{(2)}=0.711\,748$, and $E^{(3)}=0.635\,279$. Using Eqs. (18), (19), and (27)–(29), we find

$$R_H=\frac{1}{N_s e}\frac{\phi_{xy}(\tilde{\mu})E^{(2)}}{[\phi_{xx}(\tilde{\mu})E^{(1)}]^2}, \tag{31}$$

$$\Delta\rho=\frac{H^2}{2N_s\gamma_0}\frac{|\phi_M(\tilde{\mu})|E^{(3)}}{[\phi_{xx}(\tilde{\mu})E^{(1)}]^2}. \tag{32}$$

As already mentioned, the coupling of the magnetic field to the orbital motion of the electrons gives rise to a positive contribution to the resistivity.

The Hall constant (31) does not depend on the quasiparticle damping. However, the ordinary resistivity and the magnetoresistance do. Near the density-driven Mott transition, these quantities are given, due to Eq. (26), by

$$\rho=\frac{2AT^2}{N_s e^2 Z(\tilde{\mu})^2 D\phi_{xx}(\tilde{\mu})E^{(1)}}, \tag{33}$$

$$\Delta\rho=\frac{H^2 Z(\tilde{\mu})^2 D}{2N_s AT^2}\frac{|\phi_M(\tilde{\mu})|E^{(3)}}{[\phi_{xx}(\tilde{\mu})E^{(1)}]^2}. \tag{34}$$

The impact of correlations on both quantities is described by their dependence on Z: While they enhance the ordinary resistivity by a factor of $1/Z^2$, they lower the magnetoresistance by Z^2, in each case relative to a noninteracting system with the same density of states. Also, the dependences of the quantities (33) and (34) on the doping level are mainly determined by Z: As the Mott transition is approached, $\delta\to 0$, ρ diverges and the magnetoresistance vanishes. The former fact indicates that the effective charge carriers become localized. But then, the magnetic field can no longer affect the orbital motion of the electrons, hence the vanishing magnetoresistance.

Finally, the Fermi-liquid relations $\rho\propto T^2/Z^2$ and $\Delta\rho\propto Z^2/T^2$ imply the validity of Kohler's rule[23]

$$\frac{\Delta\rho}{\rho}\propto\left(\frac{H}{\rho}\right)^2. \tag{35}$$

IV. HIGH-TEMPERATURE LIMIT

To single out the contributions of the incoherent parts of the spectrum, we now consider the limit of very high temperatures. For the Hubbard interaction to retain its important impact on the electron dynamics in the high-temperature limit, we have to choose $U=\infty$ from the outset. Then, the spectral function (2) no longer receives contributions from the upper Hubbard band. We start by deriving a sum rule for the local spectral function (21). On average, each site hosts n electrons and $1-n$ holes, since $U=\infty$ means that the maximum occupancy is 1. Thus we find

$$\int_{-\infty}^{\infty} d\omega\, A(\omega)f(\omega)=n/N_s, \tag{36}$$

$$\int_{-\infty}^{\infty} d\omega\, A(\omega)[1-f(\omega)]=1-n. \tag{37}$$

These equations imply the sum rule

$$\int_{-\infty}^{\infty} d\omega\, A(\omega)=1-n+n/N_s. \tag{38}$$

Next we derive the high-temperature expansion for the chemical potential, which is defined by Eq. (36). In the limit $T\to\infty$, the spectral function (21) becomes temperature independent except for the presumably temperature-dependent peak center, $-\mu(T)$. Therefore, we introduce tilded spectral and Green's functions that are obtained from their untilded counterparts by replacing $\omega\to\omega-\mu$. For instance,

$$\tilde{A}(\omega)=A(\omega-\mu). \tag{39}$$

Equation (36) can now be rewritten as $\int_{-\infty}^{\infty}d\omega\,\tilde{A}(\omega)f(\omega-\mu)=n/N_s$. By expanding $f(\omega-\mu)$ about the peak center of $\tilde{A}(\omega)$, $\omega=0$, by further expressing all derivatives of the Fermi function by the Fermi function itself, and by using the moments

$$m_l=\int_{-\infty}^{\infty} d\omega\,\tilde{A}(\omega)\omega^l, \tag{40}$$

along with their expansion in powers of $1/T$,

$$m_l=\sum_{n=0}^{\infty}\beta^n m_l^{(n)}, \tag{41}$$

we can systematically expand $f[-\mu(T)]$ in powers of $1/T$. To first order in $1/T$, we find

$$f[-\mu(T)]=\frac{n}{N_s}\left[\frac{1}{m_0}+\beta\delta\frac{m_1^{(0)}}{m_0^3}\right]+o(\beta^2), \tag{42}$$

where $m_0=1-n+n/N_s$ according to Eq. (38).

Likewise, we can expand conductivities (4)–(6) in powers of $1/T$. In terms of the quantities

$$C_l=\int d\epsilon\,\phi_{xx}(\epsilon)\int d\omega\,\tilde{A}(\omega,\epsilon)^2\omega^l, \tag{43}$$

$$C_l^H=\int d\epsilon\,\phi_{xy}(\epsilon)\int d\omega\,\tilde{A}(\omega,\epsilon)^3\omega^l, \tag{44}$$

$$C_l^M=\int d\epsilon\,\phi_M(\epsilon)\int d\omega\,\tilde{A}(\omega,\epsilon)^4\omega^l, \tag{45}$$

which are to be calculated in the high-temperature limit, we find

$$\sigma_{xx}=N_s\pi e^2\beta A(1-A)C_0, \tag{46}$$

$$\sigma_{xy}=\frac{N_s 2\pi^2 e^3 H}{3}\beta A(1-A)[C_0^H-\beta(1-2A)C_1^H], \tag{47}$$

$$\Delta\sigma_{xx}=\frac{N_s 2\pi^3 e^4 H^2}{5}\beta A(1-A)C_0^M, \tag{48}$$

where $A\equiv(n/N_s)/(1-n+n/N_s)$. Using Eqs. (18) and (19), these results can be translated into resistivities,

$$\rho=\frac{T}{\pi e^2 N_s\zeta C_0}, \tag{49}$$

$$R_H=\frac{2(TC_0^H-\eta C_1^H)}{3eN_s\zeta C_0^2}, \tag{50}$$

$$\Delta\rho=\frac{2\pi H^2|C_0^M|}{5N_s\zeta C_0^2}T, \tag{51}$$

where we have defined $\zeta\equiv A(1-A)$ and $\eta\equiv 1-2A$, or

$$\zeta=\frac{(1-n)n/N_s}{(1-n+n/N_s)^2}. \tag{52}$$

$$\eta = \frac{1-n-n/N_s}{1-n+n/N_s}. \tag{53}$$

Before discussing these findings, we investigate the dependences of coefficients (43)–(45) on band filling and on temperature. Their doping dependence can roughly be estimated by assuming that the weight of the full spectral function [Eq. (2)] is similar to that of the local one in Eq. (21). This implies

$$C_l \approx \tilde{C}_l (1-n+n/N_s)^2, \tag{54}$$

$$C_l^H \approx \tilde{C}_l^H (1-n+n/N_s)^3, \tag{55}$$

$$C_l^M \approx \tilde{C}_l^M (1-n+n/N_s)^4, \tag{56}$$

where $\tilde{C}_l$, $\tilde{C}_l^H$, and $\tilde{C}_l^M$ are doping independent. Equations (54)–(56) can be shown to be a good approximation in the vicinity of half-filling.

The temperature dependence of coefficients (43)–(45) is more subtle because it can be affected by symmetry. C_0 and C_0^M are positive and negative definite, respectively, and therefore tend to constants determined by the limiting form of the spectral function as $T\to\infty$. However, C_0^H receives contributions of either sign, leading to the possibility that these contributions may cancel each other out in leading order due to some symmetry. As an example, we will demonstrate further down that perfect nesting leads to $C_0^H \sim 1/T$. Then both contributions in Eq. (50) matter, and the Hall constant tends to a constant as $T\to\infty$. For a general band structure, however, there is no reason why C_0^H should vanish as $T\to\infty$, so $\sigma_{xy}\sim 1/T$ like the longitudinal conductivity, and hence, $R_H \sim T$ in this limit. In the case of the simple tight-binding band of Eq. (13), we evaluate the coefficients appearing in Eqs. (49)–(51) numerically within the NCA for $\delta = 0.1$: Setting $d=3$, we find $\lim_{T\to\infty} C_0 = 1.894 \times 10^{-2}$, $\lim_{T\to\infty} T C_0^H = -2.654\times 10^{-4}$, $\lim_{T\to\infty} C_1^H = -7.602 \times 10^{-4}$, and $\lim_{T\to\infty} C_0^M = -4.529\times 10^{-4}$.

We now demonstrate that any band structure implying the symmetry properties

$$D(-\epsilon) = D(\epsilon), \tag{57}$$

$$\phi_{xy}(-\epsilon) = -\phi_{xy}(\epsilon) \tag{58}$$

in fact leads to $C_0^H \sim 1/T$. These properties can be satisfied, for instance, on account of the perfect-nesting condition

$$\epsilon(\vec{k}+\vec{Q}) = -\epsilon(\vec{k}) \tag{59}$$

for some vector $\vec{Q}$. In the case of nearest-neighbor hopping on a cubic lattice [Eq. (13)], $\vec{Q}$ is the vector pointing to the corner of the Brillouin zone, i.e., $\vec{Q} = (\pi, \pi, \ldots)$. Upon solving the dynamical mean-field equations, an even density of states as in Eq. (57) is seen to lead to an even local spectral function as $T\to\infty$:

$$\lim_{T\to\infty} \tilde{A}(-\omega) = \lim_{T\to\infty} \tilde{A}(\omega). \tag{60}$$

Finally, by again using the dynamical mean-field equations, we can show that Eq. (60) implies a symmetry property for the full spectral function:

$$\lim_{T\to\infty} \tilde{A}(-\omega, -\epsilon) = \lim_{T\to\infty} \tilde{A}(\omega, \epsilon). \tag{61}$$

Equations (58) and (61) prove that $\lim_{T\to\infty} C_0^H = 0$. The first order in $1/T$ does not vanish, hence $C_0^H \sim 1/T$ as claimed above.

We now discuss our results for the three quantities in Eqs. (49)–(51). Both the ordinary resistivity and the magnetoresistance exhibit a linear-in T behavior at high temperatures, with prefactors that diverge in the empty-band limit or as half-filling is approached. As $n\to 0$, we find $\rho, \Delta\rho \sim T/n$, which simply reflects the fact that if the charge carriers vanish, the conductivity has to vanish too. Close to half-filling, we find

$$\rho \sim T/\delta, \tag{62}$$

$$\Delta\rho \sim T/N_s^2 \delta. \tag{63}$$

At the Mott transition, these quantities diverge because localized charge carriers cannot give rise to a finite conductivity either.

The temperature dependence of the Hall constant depends on whether the given band structure satisfies conditions (57) and (58). If they are satisfied, $R_H \sim$ const, otherwise, we expect $R_H \sim T$. This result is consistent with previous works on the high-temperature Hall effect by Brinkman and Rice,[24] Oguri and Maekawa,[25] and Shastry, Shraiman, and Singh.[10] The high-temperature expansions of all these works were carried out for a cubic lattice with nearest-neighbor hopping. Therefore, they all obtained $\sigma_{xy}\sim 1/T^2$, leading to a temperature-independent Hall constant at high temperatures. Our analysis shows that this result is not generic. Rather, we expect $\sigma_{xy}\sim 1/T$ and thus $R_H \sim T$ for a general band structure at high temperatures. To check this, we calculate the infinite-frequency Hall constant R_H^* of Ref. 10 to leading order in $1/T$ on a two-dimensional cubic lattice where electrons can hop with amplitudes t and $t^{(d)}$ to, respectively, nearest-neighbor sites and diagonally across the unit cell. In essence, R_H^* is given by $\langle [\hat{J}_x, \hat{J}_y] \rangle$. For this quantity to be of order $1/T$ rather than $1/T^2$, electrons must be able to circumscribe a finite area enclosing a finite flux with just three hops. This is made possible by the inclusion of diagonal hops $t^{(d)}$. To leading order in $1/T$,[26] we find $R_H^* = [6t^2 t^{(d)}/(t^2 + 2t^{(d)2})^2][(1+\delta)T/e\,\delta(1-\delta)]$. A high-temperature behavior $R_H \sim T$ is also striking from the viewpoint of conventional band theory, where a temperature dependence can only arise below a scale set by the Debye temperature.

As for the doping dependence of the Hall constant, we find either $R_H \sim 1/N_s \delta |e|$ or $R_H \sim T/N_s \delta |e|$ close to half-filling. In any case, the Hall constant exhibits a $1/\delta$ behavior. The sign of the Hall constant is governed by the coefficients C_0^H and C_1^H. As can be seen from Eq. (44), they are a combined result of the band structure, entering via function (8), and the correlations, taken into account by the spectral function. In the case of the simple tight-binding band (13), the Hall constant is positive in the vicinity of half-filling.

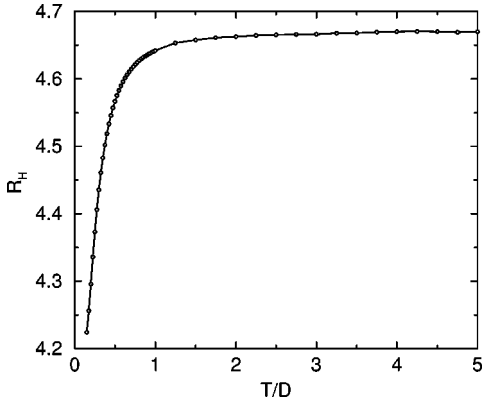

FIG. 1. Hall constant at $U=\infty$ and $\delta=0.1$.

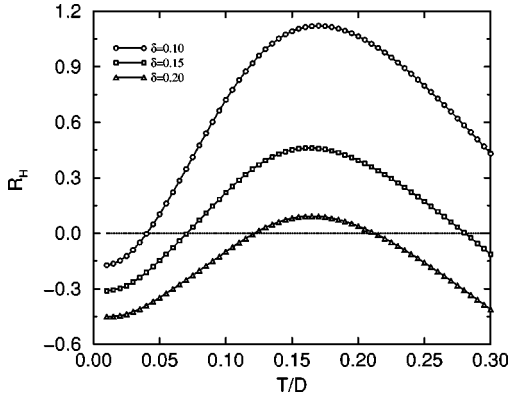

FIG. 2. Hall constant at $U=2.82$ for various doping levels.

Finally, Eqs. (62) and (63) indicate that Kohler's rule is replaced by $\Delta\rho/\rho\sim\text{const}\times H^2$ in the high-temperature limit. Moreover, the Hall angle, defined by $\cot\theta_H=\rho/R_H$, increases at most as $\cot\theta_H\sim T$ as a function of temperature, if the symmetry properties (57) and (58) are satisfied. Otherwise, $\cot\theta_H\sim$const.

V. INTERMEDIATE TEMPERATURES

The behavior of the Hall coefficient at intermediate temperatures and for some values of the parameter U were studied numerically in Refs. 8 and 9. In these works, it was stressed that the Hubbard model in infinite dimensions reproduces many observable features of the high-temperature superconductors. Other works have shown, however, that important quantities of these systems such as the specific heat are not properly described within the infinite-d Hubbard model, and that this model is more appropriate for describing some transition-metal oxides where, due to the orbital degeneracy, short-ranged magnetic correlations are weaker than in the cuprates. Nevertheless, given that we do not yet understand the physics of the cuprates, we feel that the observation of similarities between experimental results on the Hall effect in cuprates and numerical results for the infinite-d Hubbard model deserves further investigation. The magnetoresistance is a second probe of the effects of a magnetic field. In this section, we carry out a comparative study of these two quantities with the goal of elucidating which elements of the physics of the large-d Hubbard model result in the observed similarities with the cuprates. To this effect, we restrict the discussion to the simple band structure (13).

The Hall constant is shown in Figs. 1–3: We know from Sec. III that the Hall constant starts at its noninteracting value at $T=0$. We also know that within the infinite-U Hubbard model, it rapidly converges to a positive value beyond the high-energy scale D (cf. Fig. 1). Moreover, this positive value goes like $1/\delta$ in the vicinity of half-filling. In between these limiting cases, we expect a smooth crossover, implying a sign change of the Hall constant as a function of temperature. At finite U, however, the Hall constant goes through a maximum as a function of temperature (Figs. 2 and 3). For large enough U and small enough doping levels, this maximum is positive. For temperatures greater than the Mott-Hubbard gap, the dynamics of the electrons is increasingly insensitive to the interaction U, which is why the Hall constant becomes electronlike again at very high temperatures. The position of the maximum depends only weakly on the doping level and is roughly located at $T\approx 0.16D$, which is above T^* (Figs. 2 and 3). Upon increasing U, the maximum becomes little by little more asymmetric, and ultimately approaches the $U=\infty$ form of the Hall constant discussed above. This indicates that the decrease of the Hall constant as a function of temperature beyond its maximum is due to the excitation of charge across the Mott-Hubbard gap. This does not imply that the relevant temperature scale is $U-2D$, since, in dynamical mean-field theory, the two Hubbard bands are only separated by a pseudogap.[27,20] In fact, Figs. 2 and 3 show that the relevant temperature scale of the decrease is roughly $0.1D$. At first glance, the curves of Figs. 2 and 3 bear some similarities to what is found experimentally in cuprates.[28,29] In cuprates, the width of the lower Cu band is roughly 0.5 eV, implying $0.1D\sim 250$ K. This scale does in fact roughly characterize the experimentally observed decrease.[29] Yet, despite these similarities, there is a crucial difference: In cuprates, the two relevant bands are separated by a *real* gap of approximately 3 eV, which is about six times as large as the width of the lower Cu band. By contrast, in Fig. 3, these bands are separated by only a *pseudogap* which is only about as large as the width of the lower Hubbard band, namely, $U-2D=2D$. Therefore, the situation in cuprates is much closer to $U=\infty$ in our model. Given that the maximum in the Hall constant found in Ref. 8 is a finite-U effect, we conclude that the dynamical mean-field theory cannot describe the experimentally observed decrease of the Hall constant as a function of temperature un-

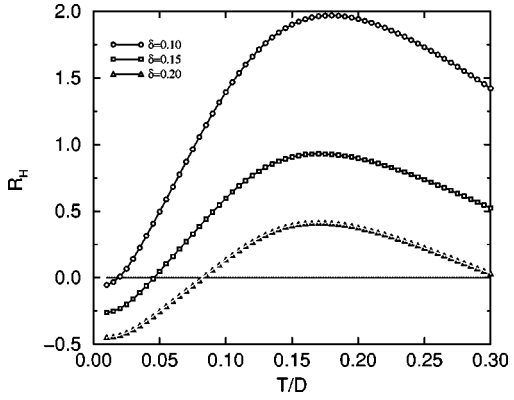

FIG. 3. Hall constant at $U=4$ for various doping levels.

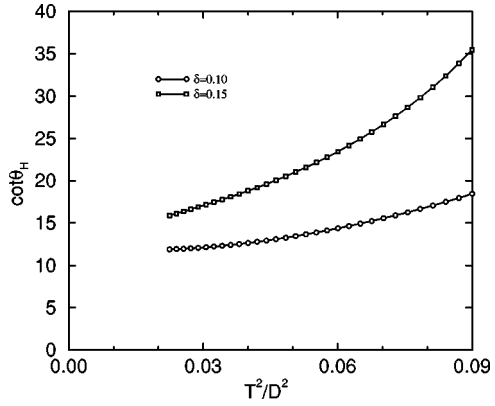

FIG. 4. Hall angle at $U=4$ for two doping levels.

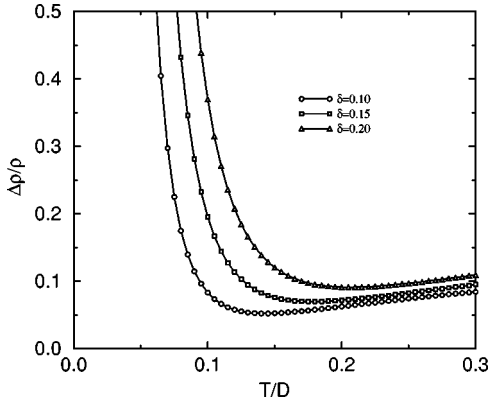

FIG. 6. $\Delta\rho/\rho$ vs temperature at $U=4$ for various doping levels.

less a reason is found to introduce a much smaller Hubbard gap within the framework of the large-d Hubbard model than what is really observed experimentally.

We now turn to the Hall angle. From our analytical investigation, we know that $\cot\theta_H \sim T$ for $T>D$ and $\cot\theta_H \sim T^2$ for $T<T_{\rm coh}$. In cuprates such as $La_{2-x}Sr_xCuO_4$, a quadratic temperature dependence of the Hall angle is observed in the underdoped compounds,[30] where at the same time the Hall constant is holelike. In Figs. 4 and 5, the Hall angle is shown as a function of T^2 in the intermediate-temperature regime, $0.15D \leqslant T \leqslant 0.3D$, where the Hall constant is positive. Figure 4 shows that $\cot\theta_H$ becomes smaller upon decreasing the doping level, as seen in the experiment.[29] However, none of the curves displays a linear behavior, although a linear fit becomes better as $U\to\infty$ and for sufficiently small temperatures and doping levels (Fig. 5). Note that a linear extrapolation of the $U=\infty$ curve in Fig. 5 would lead to a finite intercept.

Further evidence that the infinite-d Hubbard model in the intermediate-temperature regime is not able to explain the magnetotransport observed in cuprates is provided by our study of the magnetoresistance. In the Fermi-liquid regime $T<T_{\rm coh}$, we obtained $\Delta\rho/\rho \sim 1/T^4$, while in the opposite limit, at very high temperatures, this ratio saturates to a temperature-independent value. Figure 6 displays $\Delta\rho/\rho$ at $U=4$ for intermediate temperatures. Experimentally, a $1/T^4$ dependence is observed in the normal state of high-purity cuprates.[31] In contrast, the curves of Fig. 6 increase as a function of temperature in the regime where the Hall constant decreases as a function of temperature. This fact is related to the appearance of a minimum whose location depends on the doping level and which is also a finite-U effect. In fact, as can be seen in Fig. 7, this minimum is absent at $U=\infty$. There, in agreement with our analytical prediction, the ratio $\Delta\rho/\rho$ approaches a constant value beyond the high-energy scale D and cannot, therefore, obey Kohler's rule nor the modified version thereof suggested by Terasaki *et al.*[32] This is also true at intermediate temperatures.

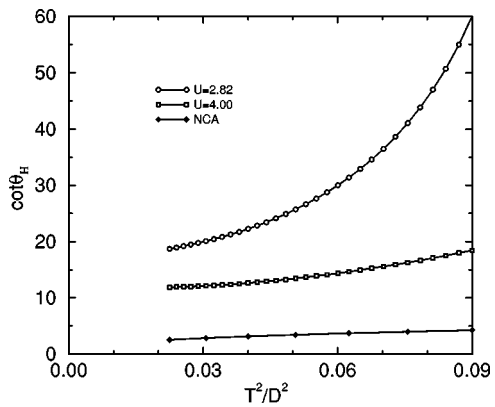

FIG. 5. Hall angle for various U and $\delta=0.1$. The NCA curve corresponds to $U=\infty$.

VI. CONCLUSIONS

In summary, we have studied the Hall effect and magnetoresistance close to the density-driven Mott transition within the single-band Hubbard model in infinite dimensions. We have shown that the orbital magnetoresistance is always nonnegative in this approximation. To elucidate the emerging dependences on temperature, on the doping level, and on the correlation strength, we have analytically considered the asymptotic regimes at very low and high temperatures. We have interpolated between these limiting cases by also computing all considered observables numerically.

In the Fermi-liquid regime, we found that correlations suppress the magnetoresistance $\Delta\rho$ by a factor Z^2, where Z is the quasiparticle residue which is linear in doping close to the Mott transition. Moreover, we have derived $\Delta\rho \sim 1/T^2$. We found that Kohler's rule is obeyed only in this low-temperature regime.

For temperatures greater than the half-band-width D but

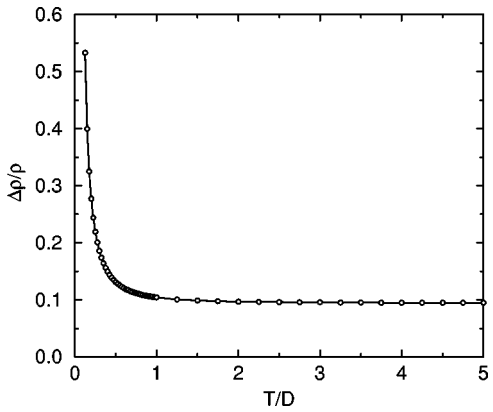

FIG. 7. $\Delta\rho/\rho$ as a function of T at $U=\infty$ and $\delta=0.1$.

much smaller than the Mott-Hubbard gap (which, therefore, was assumed to be infinite), we have obtained the following analytical results: First, the zero-field resistivity ρ and the magnetoresistivity are linear in temperature, and diverge as $1/\delta$ close to the Mott transition. Hence $\Delta\rho/\rho \sim$ const, which replaces Kohler's rule. Second, the Hall constant always diverges as $1/\delta$ close to half-filling. Finally, we have pointed out that the high-temperature behavior of the Hall effect crucially depends on the band structure: Generically, both the longitudinal and Hall conductivities go like $1/T$. This implies that the Hall constant displays a linear-in-T behavior, and the Hall angle $\cot\theta_H$ saturates as $T\to\infty$. If, on the other hand, a bipartite-lattice condition is satisfied, $R_H \sim$ const and $\cot\theta_H \sim T$.

In the intermediate-temperature regime, we have investigated the Hall constant, the Hall angle, and the magnetoresistance numerically. We have argued that none of the resulting temperature dependences can account for what is observed experimentally in the normal state of the cuprate superconductors. On the other hand, direct comparison with experiment has shown that the dynamical mean-field theory provides a surprisingly accurate description of three-dimensional transition-metal oxides,[7] and our results should serve as a qualitative guide for what we would expect in these systems.

ACKNOWLEDGMENTS

We are grateful to Gunnar Pálsson for valuable discussions. This work was supported by the NSF, Contract No. DMR 95-29138. E.L. was funded by the Deutsche Forschungsgemeinschaft.

[1] J. Hubbard, Proc. R. Soc. London, Ser. A **276**, 238 (1963).
[2] M. C. Gutzwiller, Phys. Rev. Lett. **10**, 159 (1963).
[3] J. Kanamori, Prog. Theor. Phys. **30**, 257 (1963).
[4] P. Fulde, *Electron Correlations in Molecules and Solids* (Springer, Berlin, 1991).
[5] E. Müller-Hartmann, Z. Phys. B **74**, 507 (1989).
[6] A. Khurana, Phys. Rev. Lett. **64**, 1990 (1990).
[7] A. Georges, G. Kotliar, W. Krauth, and M. J. Rozenberg, Rev. Mod. Phys. **68**, 13 (1996).
[8] T. Pruschke, M. Jarrell, and J. Freericks, Adv. Phys. **44**, 187 (1995).
[9] P. Majumdar and H. R. Krishnamurthy, cond-mat/9512151 (unpublished).
[10] B. S. Shastry, B. Shraiman, and R. R. P. Singh, Phys. Rev. Lett. **70**, 2004 (1993).
[11] H. Kajueter and G. Kotliar, Phys. Rev. Lett. **77**, 131 (1996).
[12] G. Pálsson and G. Kotliar, Phys. Rev. Lett. **80**, 4775 (1998).
[13] W. Metzner, Z. Phys. B **77**, 253 (1989).
[14] P. Voruganti, A. Golubentsev, and S. John, Phys. Rev. B **45**, 13 945 (1992).
[15] H. Kajueter, Ph.D. thesis, Rutgers University, Graduate School New Brunswick, NJ, 1996.
[16] P. Coleman, Phys. Rev. B **29**, 3035 (1984).
[17] T. Pruschke, D. L. Cox, and M. Jarrell, Phys. Rev. B **47**, 3553 (1993).
[18] T. A. Costi, J. Kroha, and P. Wölfle, Phys. Rev. B **53**, 1850 (1996).
[19] M. Jarrell and T. Pruschke, Z. Phys. B **90**, 187 (1993).
[20] H. Kajueter, G. Kotliar, and G. Moeller, Phys. Rev. B **53**, 16 214 (1996).
[21] A. Hewson, *The Kondo Problem to Heavy Fermions* (Cambridge University Press, New York, 1993).
[22] E. Müller-Hartmann, Z. Phys. B **76**, 211 (1989).
[23] J. Ziman, *Electrons and Phonons* (Oxford University Press, Oxford, 1960).
[24] W. Brinkman and T. Rice, Phys. Rev. B **4**, 1566 (1971).
[25] A. Oguri and S. Maekawa, Phys. Rev. B **41**, 6977 (1990).
[26] C. Thompson, Y. Yang, A. Guttmann, and M. Sykes, J. Phys. A **24**, 1261 (1991).
[27] A. Georges and W. Krauth, Phys. Rev. B **48**, 7167 (1993).
[28] For a review, see N. P. Ong, in *Physical Properties of High-Temperature Superconductors*, edited by D. M. Ginsberg (World Scientific, Singapore, 1990), Vol. 2, Chap. 7, pp. 459–507.
[29] H. Y. Hwang, B. Batlogg, H. Takagi, H. L. Kao, J. Kwo, R. J. Cava, J. J. Krajewski, and W. F. Peck, Phys. Rev. Lett. **72**, 2636 (1994).
[30] T. R. Chien, Z. Z. Wang, and N. P. Ong, Phys. Rev. Lett. **67**, 2088 (1991).
[31] J. M. Harris, Y. F. Yan, P. Matl, N. P. Ong, P. W. Anderson, T. Kimura, and K. Kitazawa, Phys. Rev. Lett. **75**, 1391 (1995).
[32] I. Terasaki, Y. Sato, S. Miyamoto, S. Tajima, and S. Tanaka, Phys. Rev. B **52**, 16 246 (1995).